NTLP 2008-02

Tenth-Order Lepton Anomalous Magnetic Moment — Second-Order Vertex Containing Two Vacuum Polarization Subdiagrams, One Within the Other

Tatsumi Aoyama,[1] Masashi Hayakawa,[2] Toichiro Kinoshita,[3] and Makiko Nio[4,*]

[1] *Institute of Particle and Nuclear Studies, High Energy Accelerator Research Organization (KEK), Tsukuba, Ibaraki 305-0801, Japan*

[2] *Department of Physics, Nagoya University, Nagoya, Japan 464-8602*

[3] *Laboratory for Elementary-Particle Physics, Cornell University, Ithaca, New York, 14853, U.S.A*

[4] *Theoretical Physics Laboratory, Nishina Center, RIKEN, Wako, Japan 351-0198*

(Dated: December 17, 2008)

Abstract

This paper reports the tenth-order QED contribution to the $g-2$ of electron and muon from two gauge-invariant sets, Set I(g) and Set I(h). In the case of electron $g-2$ Set I(g) consists of nine Feynman diagrams which have a fourth-order vacuum-polarization loop containing another fourth-order vacuum-polarization loop. Set I(h) consists of 30 Feynman diagrams which have a proper sixth-order vacuum-polarization loop containing a second-order vacuum-polarization loop. The results of numerical integration, including mass-dependent terms containing one closed loop of muon, are 0.028 597 (4) $(\alpha/\pi)^5$ for Set I(g) and 0.001 685 (13) $(\alpha/\pi)^5$ for Set I(h), respectively. We also report the contributions of Set I(g) and Set I(h) to the muon anomaly. Diagrams included are those containing electron, muon, and tau-lepton loops. Their sums are 2.640 9 (4)$(\alpha/\pi)^5$ and -0.564 8 (11)$(\alpha/\pi)^5$, respectively. The sum of contributions of Sets I(g) and I(h) containing only electron loops are in fair agreement with the recently obtained asymptotic analytic results.

PACS numbers: 13.40.Em, 14.60.Cd, 12.20.Ds

*Electronic address: nio@riken.jp

I. INTRODUCTION

The anomalous magnetic moment g–2 of the electron has played the central role in testing the validity of QED. To match the precision of the recent measurement of the electron $g-2$ [1], the theory must include the radiative correction of up to the eighth-order [2, 3], the hadronic contribution [4, 5, 6, 7], and the electroweak contribution [8, 9, 10] within the context of the Standard Model. As a matter of fact, the largest theoretical uncertainty now comes from the not-yet-calculated tenth-order term. Thus, for a more stringent test of QED, it is necessary to know, not a crude estimate made in Ref. [11], but an actual value of the tenth-order term. To meet this challenge we launched several years ago a systematic program to evaluate the complete tenth-order term [12, 13, 14].

The tenth-order QED contribution to the anomalous magnetic moment of an electron can be written as

$$a_e^{(10)} = \left(\frac{\alpha}{\pi}\right)^5 \left[A_1^{(10)} + A_2^{(10)}(m_e/m_\mu) + A_2^{(10)}(m_e/m_\tau) + A_3^{(10)}(m_e/m_\mu, m_e/m_\tau)\right]. \quad (1)$$

The contribution to the mass-independent term $A_1^{(10)}$ may be classified into six gauge-invariant sets, further divided into 32 gauge-invariant subsets depending on the nature of closed lepton loop subdiagrams. Thus far, results of numerical evaluation of 18 gauge-invariant subsets, which consist of 964 vertex diagrams, have been published [12, 15]. Some of 18 subsets were also analytically calculated [16] and show good agreement with the numerical results. Several more gauge-invariant sets have been evaluated and are being prepared for publication.

In this paper we report the contribution to $A_1^{(10)}$ from two gauge-invariant subsets, called Set I(g) and Set I(h). Set I(g) consists of diagrams which contain 4th-order vacuum-polarization diagrams $\Pi^{(4)}$ whose internal photon line has an insertion of another 4th-order vacuum-polarization loop. This is denoted as $\Pi^{(4,4)}$. (See Fig. 1.) Set I(h) consists of diagrams which contain proper 6th-order vacuum-polarization diagrams $\Pi^{(6)}$ in whose internal photon lines a second-order vacuum-polarization loop is inserted. This is denoted as $\Pi^{(6,2)}$. (See Fig. 2.)

The evaluation of the contributions of Set I(g) and Set I(h) to $a_e^{(10)}$ is straightforward if the spectral functions of $\Pi^{(4,4)}$ and $\Pi^{(6,2)}$ are known, since contributions of these vacuum-polarization loops can be regarded as superpositions of the second-order $g-2$ in which

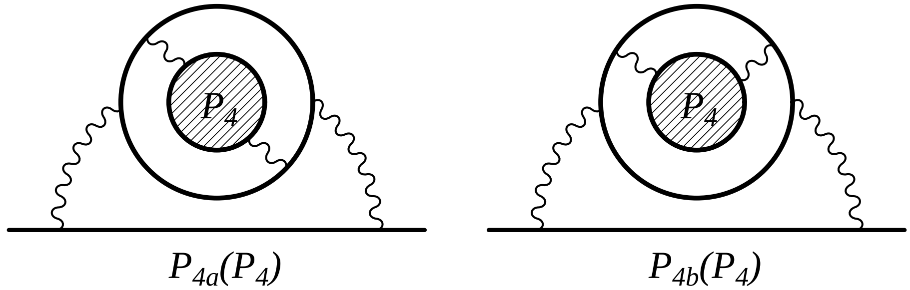

FIG. 1: Typical diagrams of Set I(g) which contain eighth-order vacuum-polarization subdiagrams $\Pi^{(4,4)}(q^2)$. Nine diagrams belong to this set.

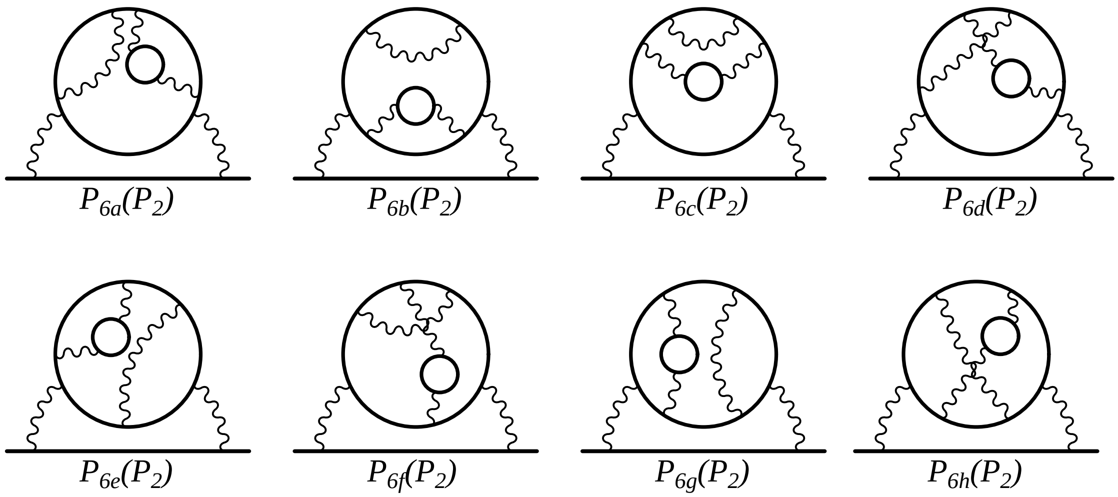

FIG. 2: Typical diagrams of Set I(h) which contain eighth-order vacuum-polarization diagrams $\Pi^{(6,2)}(q^2)$. Thirty diagrams belong to this set.

the virtual photon is replaced by massive vector bosons whose distribution is weighted by the spectral function. Unfortunately this approach is not fully applicable to our problem since exact spectral functions are known only for $\Pi^{(2)}$, $\Pi^{(4)}$ [17], and $\Pi^{(4,2)}$ [18]. Instead of pursuing the photon spectral function, we therefore follow an alternative approach [19] in which eighth-order vacuum-polarization functions $\Pi^{(4,4)}$ and $\Pi^{(6,2)}$ are constructed from Feynman-parametric integrals of $\Pi^{(4)}$ and $\Pi^{(6)}$, which are then inserted in the virtual photon line of the Feynman-parametric integral of the second-order anomalous magnetic moment $M^{(2)}$. This procedure leads to the formula [19]

$$M_{2,P} = -\int_0^1 dy(1-y)\Pi\left(q^2\right)|_{q^2=-\frac{y^2}{1-y}}, \tag{2}$$

where $\Pi(q^2)$ represents the vacuum-polarization function inserted into the photon propagator

with the momentum q.

There are two ways to construct $\Pi^{(4,4)}$. One is to treat the entire eighth-order function by direct Feynman parametrization. Another is to insert the exact fourth-order spectral function of $\Pi^{(4)}$ [17] in the Feynman-parametric integral of $\Pi^{(4)}$. We choose the second approach in this paper.

For Set I(h) an exact spectral function is not yet known. Thus we follow the alternative approach [19] which utilizes the parametric representation of the vacuum-polarization function $\Pi^{(6)}$ itself. Since the parametric integral of $\Pi^{(6)}$ is known [19], it is easy to obtain $\Pi^{(6,2)}$ by insertion of the second-order vacuum-polarization function or its spectral function in $\Pi^{(6)}$. For simplicity we choose the latter approach.

Renormalization of the vacuum-polarization function is carried out in two steps. The first step is to remove the UV divergences coming from subdiagrams of the vacuum-polarization function by the K-operation [19], supplemented by the R-subtraction [14] for some diagrams. Then a UV-finite correction, called residual renormalization, is applied to achieve the standard on-the-mass-shell renormalization.

Diagrams discussed in this paper consist of an open lepton line (l_1), a closed lepton line (l_2), and another closed lepton line (l_3) inserted in an internal photon line of (l_2), where (l_i) represents electron (e), muon (m), or tau lepton (t). Thus each diagram is characterized by a superscript ($l_1 l_2 l_3$). Residual renormalization constants are also denoted by superscripts such as ($l_2 l_3$), where l_2 is an external lepton line and l_3 refers to the inner loop.

The evaluation of Set I(g) is described in Sec. II. The evaluation of Set I(h) is described in Sec. III. Sec. IV is devoted to the summary and discussion of our results. For simplicity the factor $(\alpha/\pi)^5$ is omitted in Secs. II and III.

II. SET I(g)

In this section we consider Set I(g). The renormalized contribution of Set I(g) to the magnetic moment of the lepton l_1 is given by the general formula [19]

$$a_{l_1}^{(10)}[\mathrm{I}(g)^{(l_1 l_2 l_3)}] = \Delta M_{2,P4a(P4)}^{(l_1 l_2 l_3)} + 2\Delta M_{2,P4b(P4)}^{(l_1 l_2 l_3)} - 2\Delta B_{2,P4}^{(l_2 l_3)} M_{2,P2}^{(l_1 l_2)}, \tag{3}$$

where the first two terms are finite integrals obtained by the K-operation and the last term is the residual renormalization term.

A. Set $\mathrm{I}(g)^{(eee)}$

Let us first consider the case where l_1, l_2, l_3 are all electron lines, namely $(l_1l_2l_3) = (eee)$:

$$a_e^{(10)}[\mathrm{I}(g)^{(eee)}] = \Delta M_{2,P4a(P4)}^{(eee)} + 2\Delta M_{2,P4b(P4)}^{(eee)} - 2\Delta B_{2,P4}^{(ee)} M_{2,P2}^{(ee)}. \tag{4}$$

This gives a mass-independent contribution to the electron $g-2$. The numerical values of $\Delta M_{2,P4a(P4)}^{(eee)}$ and $\Delta M_{2,P4b(P4)}^{(eee)}$ obtained by the Monte Carlo integration routine VEGAS [20] are listed in Table I and those of $\Delta B_{2,P4}^{(ee)}$ and $M_{2,P2}^{(ee)}$ are listed in Table II. Inserting these values in Eq. (4) we obtain

$$a_e^{(10)}[\mathrm{I}(g)^{(eee)}] = 0.028\ 569\ (6). \tag{5}$$

B. Set $\mathrm{I}(g)^{(eem)}$

The contribution of Set $\mathrm{I}(g)$ to a_e, in which the inner vacuum-polarization consists of muon loop, is given by

$$a_e^{(10)}[\mathrm{I}(g)^{(eem)}] = \Delta M_{2,P4a(P4)}^{(eem)} + 2\Delta M_{2,P4b(P4)}^{(eem)} - 2\Delta B_{2,P4}^{(em)} M_{2,P2}^{(ee)}, \tag{6}$$

where the numerical values of $\Delta M_{2,P4a(P4)}^{(eem)}$ and $\Delta M_{2,P4b(P4)}^{(eem)}$ are listed in Table I and those of $\Delta B_{2,P4}^{(em)}$ and $M_{2,P2}^{(ee)}$ are listed in Table II. $m_\mu/m_e = 206.768\ 282\ 3\ (52)$ is from Ref. [11]. Inserting these values in Eq. (6) we obtain

$$a_e^{(10)}[\mathrm{I}(g)^{(eem)}] = 0.163\ 4\ (2) \times 10^{-4}. \tag{7}$$

C. Set $\mathrm{I}(g)^{(eme)}$

The contribution of Set $\mathrm{I}(g)$ to a_e, in which the outer vacuum-polarization consists of muon loop, is given by

$$a_e^{(10)}[\mathrm{I}(g)^{(eme)}] = \Delta M_{2,P4a(P4)}^{(eme)} + 2\Delta M_{2,P4b(P4)}^{(eme)} - 2\Delta B_{2,P4}^{(me)} M_{2,P2}^{(em)}, \tag{8}$$

where the numerical values of $\Delta M_{2,P4a(P4)}^{(eme)}$ and $\Delta M_{2,P4b(P4)}^{(eme)}$ are listed in Table I and those of $\Delta B_{2,P4}^{(me)}$ and $M_{2,P2}^{(em)}$ are listed in Table II. Inserting these values in Eq. (8) we obtain

$$a_e^{(10)}[\mathrm{I}(g)^{(eme)}] = 0.071\ 5\ (1) \times 10^{-4}. \tag{9}$$

Terms for (emm), (eet), etc., are even smaller than those for (eem) and (eme). Of course, they are easy to evaluate, if needed. However, they are of no physical significance at present.

TABLE I: Contributions of diagrams of Set I(g) of Fig. 1 to the electron $g-2$ with (eee), (eem), and (eme) and muon g–2 with (mee), (mem), and (mme). n_F is the number of Feynman diagrams represented by the integral. All integrals are evaluated by VEGAS [20] in double precision.

Integral	n_F	Value (Error) including n_F	Sampling per iteration	No. of iterations
$\Delta M^{(eee)}_{2,P4a(P4)}$	3	0.028 534 (5)	1×10^7	50
$\Delta M^{(eee)}_{2,P4b(P4)}$	6	0.005 798 (2)	1×10^7	50
$\Delta M^{(eem)}_{2,P4a(P4)}$	3	$0.171\ 9\ (2) \times 10^{-4}$	1×10^6	20
$\Delta M^{(eem)}_{2,P4b(P4)}$	6	$0.002\ 1\ (0) \times 10^{-4}$	1×10^6	20
$\Delta M^{(eme)}_{2,P4a(P4)}$	3	$0.052\ 2\ (1) \times 10^{-4}$	1×10^6	20
$\Delta M^{(eme)}_{2,P4b(P4)}$	6	$0.044\ 6\ (1) \times 10^{-4}$	1×10^6	20
$\Delta M^{(mee)}_{2,P4a(P4)}$	3	0.533 54 (16)	$1 \times 10^7, 1 \times 10^8$	150, 50
$\Delta M^{(mee)}_{2,P4b(P4)}$	6	2.219 96 (17)	$1 \times 10^7, 1 \times 10^8$	150, 50
$\Delta M^{(mem)}_{2,P4a(P4)}$	3	0.059 619 (60)	1×10^7	20
$\Delta M^{(mem)}_{2,P4b(P4)}$	6	0.002 157 (12)	1×10^7	20
$\Delta M^{(mme)}_{2,P4a(P4)}$	3	0.139 86 (19)	1×10^7	20
$\Delta M^{(mme)}_{2,P4b(P4)}$	6	0.131 30 (23)	1×10^7	20

D. Contribution to muon $g-2$ from Set I(g)

The leading contribution of Set I(g) to the muon anomaly a_μ comes from the diagrams in which both vacuum-polarization loops consist of electrons, namely,

$$a^{(10)}_\mu[\mathrm{I}(g)^{(mee)}] = \Delta M^{(mee)}_{2,P4a(P4)} + 2\Delta M^{(mee)}_{2,P4b(P4)} - 2\Delta B^{(ee)}_{2,P4} M^{(me)}_{2,P2}\,, \tag{10}$$

where the numerical values of $\Delta M^{(mee)}_{2,P4a(P4)}$ and $\Delta M^{(mee)}_{2,P4b(P4)}$ are listed in Table I and those of $\Delta B^{(ee)}_{2,P4}$ and $M^{(me)}_{2,P2}$ are listed in Table II. Inserting these values in Eq. (10) we obtain

$$a^{(10)}_\mu[\mathrm{I}(g)^{(mee)}] = 2.351\ 53\ (23). \tag{11}$$

TABLE II: Auxiliary integrals for Sets I(g) and I(h). Some integrals are known exactly. Other integrals are obtained by the integration routine VEGAS. The superscript $P4$ stands for the sum of the parametric constructions of the fourth-order vacuum-polarization functions $P4a$ and $P4b$. For the case of $\Delta B_{2,P4}$, the fourth-order vacuum polarization is inserted into ΔB_2 by using the Källén-Sabri spectral function. The relation between $P4$ here and the sum of $P4a$ and $P4b$ is given by $\Delta B_{2,P4} = \Delta B_{2,P4a} + \Delta B_{2,P4b} - \Delta B_2 \Delta B_{2,P2}$.

Integral	Value(Error)	Integral	Value(Error)
$M_{2,P2}^{(ee)}$	0.015 687 421...	$\Delta M_{2,P4}^{(ee)}$	0.076 401 785...
$M_{2,P2}^{(em)}$	0.005 197 (1) $\times 10^{-4}$	$\Delta M_{2,P4}^{(em)}$	0.027 526 (1) $\times 10^{-4}$
$M_{2,P2}^{(me)}$	1.094 259 6 (0)	$\Delta M_{2,P4}^{(me)}$	3.134 97 (14)
ΔB_2	0.75		
$\Delta B_{2,P2}^{(ee)}$	0.063 399 266...	$\Delta B_{2,P4}^{(ee)}$	0.183 666 5 (18)
$\Delta B_{2,P2}^{(em)}$	0.094 054 (1) $\times 10^{-4}$	$\Delta B_{2,P4}^{(em)}$	0.338 738 (12) $\times 10^{-4}$
$\Delta B_{2,P2}^{(me)}$	1.885 766 (77)	$\Delta B_{2,P4}^{(me)}$	2.438 91 (23)
$\Delta M_{2,P4(P2)}^{(eee)}$	0.013 120 (1)	$\Delta M_{2,P4(P2)}^{(eem)}$	0.047 678 (13) $\times 10^{-4}$
$\Delta M_{2,P4(P2)}^{(eme)}$	0.078 454 (8) $\times 10^{-4}$	$\Delta M_{2,P4(P2)}^{(mee)}$	1.579 51 (4)
$\Delta B_{4,P2}^{(ee)}$	−0.314 320 (10)	$\Delta L_{4,P2}^{(ee)}$	0.200 092 (14)
$\Delta B_{4,P2}^{(em)}$	−0.915 7 (47) $\times 10^{-4}$	$\Delta L_{4,P2}^{(em)}$	0.116 1 (64) $\times 10^{-4}$
$\Delta B_{4,P2}^{(me)}$	−3.420 4 (72)	$\Delta L_{4,P2}^{(me)}$	3.121 3 (63)

Contributions of terms of type (mme) and (mem) are

$$a_\mu^{(10)}[\mathrm{I}(g)^{(mme)}] = 0.194\ 64\ (29), \tag{12}$$

and

$$a_\mu^{(10)}[\mathrm{I}(g)^{(mem)}] = 0.061\ 702\ (61), \tag{13}$$

respectively.

Terms involving tau-lepton loop are three orders of magnitude smaller than (11), but greater than the uncertainty of (11). Contributions of terms of type (met), (mte), (mmt),

(mtm), and (mtt) are

$$a_\mu^{(10)}[\mathrm{I}(g)^{(met)}] = 0.001\ 236\ (2), \tag{14}$$

$$a_\mu^{(10)}[\mathrm{I}(g)^{(mte)}] = 0.001\ 485\ (4), \tag{15}$$

$$a_\mu^{(10)}[\mathrm{I}(g)^{(mmt)}] = 0.000\ 893\ (2), \tag{16}$$

$$a_\mu^{(10)}[\mathrm{I}(g)^{(mtm)}] = 0.000\ 663\ (1), \tag{17}$$

$$a_\mu^{(10)}[\mathrm{I}(g)^{(mtt)}] = 0.000\ 141\ (1), \tag{18}$$

respectively.

III. SET I(h)

For Set I(h) the formula for the renormalized quantity, including residual renormalization, takes different forms depending on whether one follows the original K-operation [19], which subtracts only the UV-divergent part of mass-renormalization constant, or the recently developed R-subtraction method [14], which subtracts the entire mass-renormalization term. We follow here the latter approach which affects the definition of $\Delta M_{2,P6i(P2)}^{(l_1 l_2 l_3)}$ for $i = c, d$. Of course, these two methods are equivalent and give the same results.

A. Set I$(h)^{(eee)}$

The renormalized contribution of Set I(h) with (eee) to a_e is given by

$$\begin{aligned} a_e^{(10)}[\mathrm{I}(h)^{(eee)}] &= \sum_{i=a}^{h} \Delta M_{2,P6i(P2)}^{(eee)} \\ &- 4\Delta B_2 \Delta M_{2,P4(P2)}^{(eee)} - 4\Delta B_{2,P2}^{(ee)} \Delta M_{2,P4}^{(ee)} \\ &+ 10\Delta B_2 \Delta B_{2,P2}^{(ee)} M_{2,P2}^{(ee)} - 2(\Delta L_{4,P2}^{(ee)} + \Delta B_{4,P2}^{(ee)}) M_{2,P2}^{(ee)}, \end{aligned} \tag{19}$$

where $\Delta M_{2,P4(P2)}^{(eee)}$, $\Delta L_{4,P2}^{(ee)}$, and $\Delta B_{4,P2}^{(ee)}$ are obtained from the lower-order relations [19]

$$\begin{aligned} \Delta M_{2,P4} &= \Delta M_{2,P4a} + 2\Delta M_{2,P4b}, \\ \Delta L_4 &= \Delta L_{4x} + 2\Delta L_{4c} + \Delta L_{4l} + 2\Delta L_{4s}. \\ \Delta B_4 &= \Delta B_{4a} + \Delta B_{4b}, \end{aligned} \tag{20}$$

by insertion of a vacuum-polarization loop $P2$ in each of two photon lines of P_{4a}, P_{4b}, ΔL_4, and ΔB_4. Substituting numerical values listed in Tables II and III in Eq. (19) we obtain

$$a_e^{(10)}[\mathrm{I}(h)^{(eee)}] = 0.001\ 696\ (13). \tag{21}$$

B. Set $\mathrm{I}(h)^{(eem)}$

The contribution of Set I(h) to a_e, in which the inner vacuum-polarization loop consists of muon, is given by

$$\begin{aligned} a_e^{(10)}[\mathrm{I}(h)^{(eem)}] &= \sum_{i=a}^{h} \Delta M_{2,P6i(P2)}^{(eem)} \\ &- 4\Delta B_2 \Delta M_{2,P4(P2)}^{(eem)} - 4\Delta B_{2,P2}^{(em)} \Delta M_{2,P4}^{(ee)} \\ &+ 10\Delta B_2 \Delta B_{2,P2}^{(em)} M_{2,P2}^{(ee)} - 2(\Delta L_{4,P2}^{(em)} + \Delta B_{4,P2}^{(em)}) M_{2,P2}^{(ee)}. \end{aligned} \tag{22}$$

Numerical values of $\Delta M_{2,P6i(P2)}^{(eem)}$ are listed in Table III, and auxiliary quantities are listed in Tables II. Inserting these values in Eq. (22) we obtain

$$a_e^{(10)}[\mathrm{I}(h)^{(eem)}] = -0.233\ 5\ (13) \times 10^{-4}. \tag{23}$$

C. Set $\mathrm{I}(h)^{(eme)}$

The contribution of Set I(h) to a_e, in which the outer vacuum-polarization consists of muon loop, is given by

$$\begin{aligned} a_e^{(10)}[\mathrm{I}(h)^{(eme)}] &= \sum_{i=a}^{h} \Delta M_{2,P6i(P2)}^{(eme)} \\ &- 4\Delta B_2 \Delta M_{2,P4(P2)}^{(eme)} - 4\Delta B_{2,P2}^{(me)} \Delta M_{2,P4}^{(em)} \\ &+ 10\Delta B_2 \Delta B_{2,P2}^{(me)} M_{2,P2}^{(em)} - 2(\Delta L_{4,P2}^{(me)} + \Delta B_{4,P2}^{(me)}) M_{2,P2}^{(em)}. \end{aligned} \tag{24}$$

Numerical values of $\Delta M_{2,P6i(P2)}^{(eme)}$ are listed in Table III, and auxiliary quantities are listed in Tables II. Inserting these values in Eq. (24) we obtain

$$a_e^{(10)}[\mathrm{I}(h)^{(eme)}] = 0.127\ 9\ (2) \times 10^{-4}. \tag{25}$$

Terms for (emm), (eet), etc. will be even smaller. Thus, they are of no physical significance at present. Of course it is easy to evaluate them, if needed.

TABLE III: Contributions of diagrams of Set I(h) of Fig.2 with (eee), (eem), and (eme). n_F is the number of Feynman diagrams represented by the integral. All integrals are evaluated in double precision.

Integral	n_F	Value (Error) including n_F	Sampling per iteration	No. of iterations
$\Delta M^{(eee)}_{2,P6a(P2)}$	4	0.003 269 (2)	1×10^8	150
$\Delta M^{(eee)}_{2,P6b(P2)}$	2	0.002 367 (2)	1×10^8	150
$\Delta M^{(eee)}_{2,P6c(P2)}$	4	−0.003 602 (2)	1×10^8	150
$\Delta M^{(eee)}_{2,P6d(P2)}$	4	−0.006 761 (3)	1×10^8	150
$\Delta M^{(eee)}_{2,P6e(P2)}$	8	0.072 639 (9)	1×10^8	150
$\Delta M^{(eee)}_{2,P6f(P2)}$	4	−0.051 169 (4)	1×10^8	150
$\Delta M^{(eee)}_{2,P6g(P2)}$	2	0.028 956 (4)	1×10^8	150
$\Delta M^{(eee)}_{2,P6h(P2)}$	2	0.003 673 (3)	1×10^8	150
$\Delta M^{(eem)}_{2,P6a(P2)}$	4	0.000 99 (7) $\times 10^{-4}$	1×10^7	50
$\Delta M^{(eem)}_{2,P6b(P2)}$	2	0.001 08 (5) $\times 10^{-4}$	1×10^7	50
$\Delta M^{(eem)}_{2,P6c(P2)}$	4	−0.006 60 (5) $\times 10^{-4}$	1×10^7	50
$\Delta M^{(eem)}_{2,P6d(P2)}$	4	−0.014 12 (14) $\times 10^{-4}$	1×10^7	50
$\Delta M^{(eem)}_{2,P6e(P2)}$	8	0.463 55 (84) $\times 10^{-4}$	1×10^7	50
$\Delta M^{(eem)}_{2,P6f(P2)}$	4	−0.476 36 (57) $\times 10^{-4}$	1×10^7	50
$\Delta M^{(eem)}_{2,P6g(P2)}$	2	0.140 65 (50) $\times 10^{-4}$	1×10^7	50
$\Delta M^{(eem)}_{2,P6h(P2)}$	2	−0.198 15 (63) $\times 10^{-4}$	1×10^7	50
$\Delta M^{(eme)}_{2,P6a(P2)}$	4	0.073 23 (7) $\times 10^{-4}$	1×10^7	50
$\Delta M^{(eme)}_{2,P6b(P2)}$	2	0.047 15 (5) $\times 10^{-4}$	1×10^7	50
$\Delta M^{(eme)}_{2,P6c(P2)}$	4	0.015 22 (6) $\times 10^{-4}$	1×10^7	50
$\Delta M^{(eme)}_{2,P6d(P2)}$	4	−0.061 12 (6) $\times 10^{-4}$	1×10^7	50
$\Delta M^{(eme)}_{2,P6e(P2)}$	8	0.398 96 (16) $\times 10^{-4}$	1×10^7	50
$\Delta M^{(eme)}_{2,P6f(P2)}$	4	−0.150 36 (5) $\times 10^{-4}$	1×10^7	50
$\Delta M^{(eme)}_{2,P6g(P2)}$	2	0.122 27 (5) $\times 10^{-4}$	1×10^7	50
$\Delta M^{(eme)}_{2,P6h(P2)}$	2	0.048 79 (4) $\times 10^{-4}$	1×10^7	50

D. Contribution to muon $g-2$ from Set I(h)

FORTRAN programs for the electron $g-2$ can be readily converted to the muon case by changing one or two parameters. In the case (mee) the renormalized contribution of Set I(h) to a_μ is given by

$$\begin{aligned} a_\mu^{(10)}[\mathrm{I}(h)^{(mee)}] &= \sum_{i=a}^{h} \Delta M_{2,P6i(P2)}^{(mee)} \\ &- 4\Delta B_2 \Delta M_{2,P4(P2)}^{(mee)} - 4\Delta B_{2,P2}^{(ee)} \Delta M_{2,P4}^{(me)} \\ &+ 10\Delta B_2 \Delta B_{2,P2}^{(ee)} M_{2,P2}^{(me)} - 2(\Delta L_{4,P2}^{(ee)} + \Delta B_{4,P2}^{(ee)}) M_{2,P2}^{(me)}. \end{aligned} \tag{26}$$

Substituting numerical values listed in Tables II and IV in Eq. (26) we obtain

$$a_\mu^{(10)}[\mathrm{I}(h)^{(mee)}] = -0.790\ 83\ (59). \tag{27}$$

Contributions of terms of type (mme) and (mem) are

$$a_\mu^{(10)}[\mathrm{I}(h)^{(mme)}] = 0.253\ 70\ (57), \tag{28}$$

and

$$a_\mu^{(10)}[\mathrm{I}(h)^{(mem)}] = -0.031\ 48\ (62), \tag{29}$$

respectively. Contributes involving tau lepton is small but not negligible. Contributions of terms of type (met), (mte), (mmt), (mtm), (mtt) are

$$a_\mu^{(10)}[\mathrm{I}(h)^{(met)}] = -0.001\ 303\ (17), \tag{30}$$

$$a_\mu^{(10)}[\mathrm{I}(h)^{(mte)}] = 0.003\ 281\ (5), \tag{31}$$

$$a_\mu^{(10)}[\mathrm{I}(h)^{(mmt)}] = -0.000\ 612\ (4), \tag{32}$$

$$a_\mu^{(10)}[\mathrm{I}(h)^{(mtm)}] = 0.000\ 746\ (2), \tag{33}$$

$$a_\mu^{(10)}[\mathrm{I}(h)^{(mtt)}] = 0.000\ 026\ (1), \tag{34}$$

respectively.

IV. SUMMARY AND DISCUSSION

The contribution of Set I(g) to the electron $g-2$, including mass-depending terms where one of lepton loops is a muon loop, is the sum of (5), (7), and (9):

$$a_e^{(10)}[\mathrm{I}(g)] = 0.028\ 592\ (6) \left(\frac{\alpha}{\pi}\right)^5. \tag{35}$$

TABLE IV: Contributions of diagrams of Set I(h) of Fig.2 to a_μ with (mee), (mem), and (mme). n_F is the number of Feynman diagrams represented by the integral. All integrals are evaluated in double precision.

Integral	n_F	Value (Error) including n_F	Sampling per iteration	No. of iterations
$\Delta M^{(mee)}_{2,P6a(P2)}$	4	4.039 70 (23)	1×10^9	200
$\Delta M^{(mee)}_{2,P6b(P2)}$	2	2.198 75 (8)	1×10^9	200
$\Delta M^{(mee)}_{2,P6c(P2)}$	4	1.738 74 (9)	1×10^9	200
$\Delta M^{(mee)}_{2,P6d(P2)}$	4	−3.303 39 (8)	1×10^9	200
$\Delta M^{(mee)}_{2,P6e(P2)}$	8	7.478 07 (29)	1×10^9	200
$\Delta M^{(mee)}_{2,P6f(P2)}$	4	−12.321 11 (19)	1×10^9	200
$\Delta M^{(mee)}_{2,P6g(P2)}$	2	−1.867 04 (23)	1×10^9	200
$\Delta M^{(mee)}_{2,P6h(P2)}$	2	6.007 99 (9)	1×10^9	200
$\Delta M^{(mem)}_{2,P6a(P2)}$	4	0.003 32 (13)	1×10^7	50
$\Delta M^{(mem)}_{2,P6b(P2)}$	2	0.002 236 (77)	1×10^7	50
$\Delta M^{(mem)}_{2,P6c(P2)}$	4	0.002 148 (25)	1×10^7	50
$\Delta M^{(mem)}_{2,P6d(P2)}$	4	−0.000 639 (80)	1×10^7	50
$\Delta M^{(mem)}_{2,P6e(P2)}$	8	0.289 64 (50)	1×10^7	50
$\Delta M^{(mem)}_{2,P6f(P2)}$	4	−0.231 04 (18)	1×10^7	50
$\Delta M^{(mem)}_{2,P6g(P2)}$	2	−0.047 18 (51)	1×10^7	50
$\Delta M^{(mem)}_{2,P6h(P2)}$	2	0.014 71 (7)	1×10^7	50
$\Delta M^{(mme)}_{2,P6a(P2)}$	4	0.206 70 (19)	1×10^7	50
$\Delta M^{(mme)}_{2,P6b(P2)}$	2	0.134 50 (15)	1×10^7	50
$\Delta M^{(mme)}_{2,P6c(P2)}$	4	0.036 45 (14)	1×10^7	50
$\Delta M^{(mme)}_{2,P6d(P2)}$	4	−0.169 33 (13)	1×10^7	50
$\Delta M^{(mme)}_{2,P6e(P2)}$	8	1.077 82 (44)	1×10^7	50
$\Delta M^{(mme)}_{2,P6f(P2)}$	4	−0.451 81 (13)	1×10^7	50
$\Delta M^{(mme)}_{2,P6g(P2)}$	2	0.281 06 (11)	1×10^7	50
$\Delta M^{(mme)}_{2,P6h(P2)}$	2	0.146 48 (9)	1×10^7	50

The contribution of Set I(h) to the electron $g-2$, including mass-depending terms where one of lepton loops is a muon loop, is the sum of (21), (25), and (23):

$$a_e^{(10)}[\mathrm{I}(h)] = 0.001\ 685\ (13) \left(\frac{\alpha}{\pi}\right)^5 . \tag{36}$$

Thus the contributions of Set I(g) and Set I(h) to the electron $g-2$ are small and within computational uncertainties of several other gauge-invariant sets [2].

The contribution of Set I(g) to the muon $g-2$, including terms where lepton loops are electrons, an electron and a muon, an electron and a tau lepton, or muon loops, is the sum of (11), (12), (13), (14), (15), (16), (17), (18), and (5):

$$a_\mu^{(10)}[\mathrm{I}(g)] = 2.630\ 86\ (37) \left(\frac{\alpha}{\pi}\right)^5 , \tag{37}$$

noting that Eq. (5) holds for the case (mmm), too.

The contribution of Set I(h) to the muon $g-2$, including terms where lepton loops are electrons, an electron and a muon, an electron and a tau lepton, or muon loops, is the sum of (27), (28), (29), (30), (31), (32), (33), (34), and (21):

$$a_\mu^{(10)}[\mathrm{I}(h)] = -0.564\ 8\ (11) \left(\frac{\alpha}{\pi}\right)^5 , \tag{38}$$

noting that Eq. (21) holds for the case (mmm), too.

Thus the contributions of Sets I(g) and I(h) to the muon g–2 are also very small compared with the total contribution 663 (20) $(\alpha/\pi)^5$ of 18 gauge-invariant sets, which include all dominant terms containing light-by-light-scattering subdiagrams and/or vacuum-polarization subdiagrams [12]. Concerning the total contribution to the muon $g-2$, see also [21].

Recently an analytic value of the asymptotic contribution of the sum of Set I(g) and Set I(h) to a_μ has been obtained:[22]

$$a_\mu^{(10)}[\mathrm{I}(g+h)^{(mee)} : \text{analytic-asymptotic}] = 1.501\ 12 \left(\frac{\alpha}{\pi}\right)^5 . \tag{39}$$

This is in fair agreement with our result

$$a_\mu^{(10)}[\mathrm{I}(g+h)^{(mee)}] = 1.560\ 70\ (64) \left(\frac{\alpha}{\pi}\right)^5 . \tag{40}$$

Note, however, that the difference between (39) and (40) is 93 times larger than the estimated uncertainty of numerical integration. This may be attributed to the $\mathcal{O}(m_e/m_\mu)$ term not included in the analytic result.

Acknowledgments

This work is supported in part by JSPS Grant-in-Aid for Scientific Research (C) No. 19540322. T. K.'s work is supported by the U. S. National Science Foundation Grant No. PHY-0355005. T. K. thanks RIKEN for the hospitality extended to him while part of this work was carried out. M. H. is also supported in part by JSPS Grant-in-Aid for Scientific Research (C) No. 20540261. Numerical computations were partly conducted on the RIKEN Super Combined Cluster System (RSCC).

---

[1] D. Hanneke, S. Fogwell, and G. Gabrielse, Phys. Rev. Lett. **100**, 120801 (2008).

[2] T. Kinoshita and M. Nio, Phys. Rev. D **73**, 013003 (2006).

[3] T. Aoyama, M. Hayakawa, T. Kinoshita, and M. Nio, Phys. Rev. Lett. **99**, 110406 (2007); Phys. Rev. D **77**, 053012 (2008).

[4] M. Davier and A. Höcker, Phys. Lett. **B419**, 419(1998); M. Davier, in Proceedings of the International Workshop on Tau Lepton Physics (Tau08), Novosibirsk, Russia, 22-25 September 2008 (unpublished).

[5] K. Hagiwara, A. D. Martin, D. Nomura, and T. Teubner, Phys. Lett. **B649**, 173 (2007).

[6] B. Krause, Phys. Lett. **B390**, 392 (1997).

[7] K. Melnikov and A. Vainshtein, Phys. Rev. D **70**, 113006 (2004); M. Davier and W. J. Marciano, Ann. Rev. Nucl. Part. Sci. **54**, 115 (2004); J. Bijnens and J. Prades, Mod. Phys. Lett. **A22**, 767 (2007).

[8] A. Czarnecki, B. Krause, and W. J. Marciano, Phys. Rev. Lett. **76**, 3267 (1996).

[9] M. Knecht, S. Peris, M. Perrottet, and E. de Rafael, J. High Energy Phys. **11**, 003 (2002).

[10] A. Czarnecki, W. J. Marciano, and A. Vainshtein, Phys. Rev. D **67**, 073006 (2003).

[11] P. J. Mohr, B. N. Taylor, and D. B. Newell, Rev. Mod. Phys. **80**, 633 (2008).

[12] T. Kinoshita and M. Nio, Phys. Rev. D **73**, 053007 (2006).

[13] T. Aoyama, M. Hayakawa, T. Kinoshita, and M. Nio, Nucl. Phys. B **740**, 138 (2006).

[14] T. Aoyama, M. Hayakawa, T. Kinoshita, and M. Nio, Nucl. Phys. B **796**, 184 (2008).

[15] T. Aoyama, M. Hayakawa, T. Kinoshita, M. Nio, and N. Watanabe, Phys. Rev. D **78**, 053005 (2008).

[16] S. Laporta, Phys. Lett. **B328**, 522 (1994).

[17] G. Källén and A. Sabri, Dan. Vidensk. Selsk. Mat.-Fys. Medd. **29**, 17 (1955).

[18] A. H. Hoang, J. H. Kühn, and T. Teubner, Nucl. Phys. **B452**, 173 (1995).

[19] T. Kinoshita, *Theory of the Anomalous Magnetic Moment of the Electron - Numerical Approach* in *Quantum Electrodynamics*, edited by T. Kinoshita (World Scientific, Singapore, 1990), pp. 218 - 321.

[20] G. P. Lepage, J. Comput. Phys. **27**, 192 (1978).

[21] A. L. Kataev, Phys. Rev. D **74**, 073011(2006).

[22] P. A. Baikov, K. G. Chetyrkin, and C. Sturm, Nucl. Phys. B, Proc. Suppl. **183**, 8 (2008); K. Chetyrkin, talk presented at the Loops and Legs Conference 2008.